

Real-time segmentation of blood vessels, nerves and bone in ultrasound-guided regional anesthesia using deep learning

Erik Smistad^{*†}, Torgrim Lie^{*}, Kaj Fredrik Johansen[‡]

^{*}SINTEF Medical Technology

Trondheim, Norway

[†]Norwegian University of Science and Technology (NTNU)

Dept. of Circulation and Medical Imaging

Trondheim, Norway

[‡]St. Olavs Hospital, Clinic of Anaesthesia and Intensive care

Trondheim, Norway

Abstract—Images from ultrasound-guided regional anesthesia procedures can be difficult to interpret, especially by non-experts.

In this work, deep convolutional neural networks were used to segment blood vessels, nerves and bone from two different nerve block procedures; the axillary nerve block and the femoral nerve block, which are commonly used to block sensation of pain from arms and legs respectively.

The results show that the detection performance vary a lot for different nerves, with the best F1 and Dice scores of 0.84 and 0.67 for the median nerve, and the worst score of 0.54 and 0.51 for the ulnar nerve. Blood vessels and bone are generally easy to detect, but small veins can be difficult to segment accurately.

Using the trained neural networks, a portable prototype system able to stream, process and visualize the results in real-time was created using a laptop, the FAST framework, and a Clarius L15 HD scanner. The runtime was measured to be about 31 milliseconds per frame.

I. INTRODUCTION

Ultrasound-guided nerve block procedures are commonly used to block sensations of pain from body parts such as arms and legs, as an alternative to general anesthesia. Ultrasound imaging is used to find the target nerves and the surrounding blood vessels, and to guide the needle used to inject local anesthetics around the nerves.

Ultrasound images of these procedures can be difficult to interpret, especially for non-experts. Worm et al. [1] concluded that ultrasound-guided regional anesthesia education focusing on still ultrasound images is not sufficient, while ultrasound videos and graphical enhancers may aid students in learning to identify nerves in ultrasound. Wegener et al. [2] did an experiment with 35 novice subjects, who had performed less than 30 ultrasound guided nerve blocks, on identification of nerves and related structures in ultrasound images from several locations. They observed that after a basic training course, one group of the participants failed to identify more than half of the anatomical structures, while the other group, which received an additional tutorial, failed to identify a third of the structures. These low identification scores of non-experts indicate that there is a need for better training tools. Nerves are often

difficult to distinguish from other types of tissue in ultrasound images. In general, nerves appear as bright structures with black spots inside, but can vary a lot depending on their location and surrounding tissue.

Our goal is to use image segmentation to highlight and label nerves, as well as surrounding structures such as blood vessels and bone, using deep neural networks in real-time while scanning to help non-experts.

Segmentation of nerves in ultrasound images has been studied in several publications over the last decade. Hadjerci et al. [3] segmented the median nerve of the lower arm from ultrasound images using k-means clustering to find hyperechoic tissue, then a texture analysis method using a support vector machine classifier to identify the nerve. Hadjerci et al. developed this method further in [4] and [5]. A segmentation method for the sciatic nerve in the back of the leg in ultrasound images was presented by Hafiane et al. [6]. This method involved active contour segmentation driven by a phase-based probabilistic gradient vector flow. Smistad et al. [7] created a guidance system for femoral nerve blocks where the femoral artery and nerve was automatically segmented in real-time. This system used a combination of the location of the artery, fascia and presence of hyperechoic tissue to infer the location of the femoral nerve.

The short axis cross section of blood vessels usually appear as dark ellipses in an ultrasound image. Several tracking methods using Kalman filters have been proposed [8], [9], [10]. Most of these methods require manual initialization, and are sensitive to user settings such as gain on the ultrasound scanner.

In recent years, deep convolutional neural networks (CNNs) have achieved great results in image classification, segmentation and object detection, even on challenging ultrasound images. CNNs have also been used to find the nerves in ultrasound images. In 2017, Zhao and Sun [11], and Baby and Jereesh [12] used a U-net type CNN on the Kaggle dataset on ultrasound images of nerves in the neck. The

appearance of nerves vary a lot depending on the patient and the location in the body. Creating a segmentation method which can accurately find nerves anywhere in the body is challenging and unsolved. All previous studies therefore target specific nerves. CNNs have also been used to find blood vessels in ultrasound images. Smistad et al. [13] used an image classification network to classify image patches of vessel-like structures. In 2018, Smistad et al. [14] used a U-net type CNN to segment different nerves and blood vessels from ultrasound images of the armpit and demonstrated the benefits of using image augmentations to improve the accuracy.

In this work, we have targeted two common ultrasound-guided regional anesthesia procedures; the axillary and femoral nerve blocks which are used to block nerves in arms and legs respectively. Compared to previous work, our deep learning method can segment multiple different nerves, blood vessels and bone in real-time. Using the trained neural networks, a portable prototype was created which streams ultrasound images from a Clarius ultrasound scanner, and then segments and visualizes the results in real-time on a laptop.

II. METHODS

A. Data and annotation

Ultrasound videos from 108 subjects of the armpit was collected both from healthy volunteers and patients. Several different ultrasound scanners were used: Ultrasonix Sonix MDP L14-5, SonoSite M-Turbo/Edge HDL38 and Clarius L15 HD. The imaging depth varied from 2.5 to 5 cm. A smaller dataset from 20 subjects of the groin was also collected to test the method on the femoral nerve block as well.

The ultrasound videos were annotated by an expert anesthesiologist using Annotation Web [15] to delineate nerves, blood vessels and bone. For the armpit, the musculocutaneous (MSC), median and ulnar nerves were annotated, and for the groin, the femoral nerve was annotated. The ultrasound and annotation images were resized to a fixed size of 256×256 . The aspect ratio of the images were preserved by padding with zero or cropping at the bottom of the images.

B. Neural network architecture

The CNN architecture used in this study was a fully-convolutional encoder-decoder U-net type network [16]. This architecture has six levels with cross-over connections and uses 2×2 max pooling in the encoder and 2×2 repeat upsampling in the decoder. Two 3×3 convolution layers are used at each level, together with ReLU activation. Network input is an ultrasound image of size 256×256 . The output is a segmentation of the same size as the input image. For the axillary nerve block, the network has six output channels (background, blood, bone, MSC, median and ulnar nerve), while for the femoral nerve block, there are four output channels (background, blood, bone, femoral nerve). The networks have about two million parameters and was designed for real-time use with a runtime of only a few milliseconds on a modern GPU.

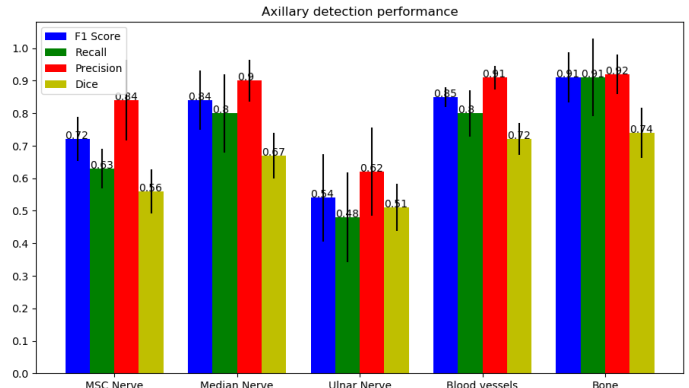


Fig. 1. Detection performance of each structure for the axillary nerve block. The black vertical lines represents the standard deviation.

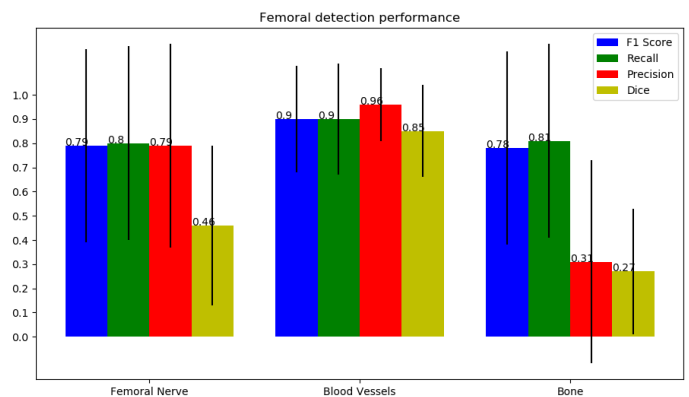


Fig. 2. Detection performance of each structure for the femoral nerve block. The black vertical lines represents the standard deviation.

C. Training

The neural networks were trained using Keras with 10-fold cross-validation, Adam optimizer, 150 epochs and a Dice loss function. Random augmentations were used during training to reduce overfitting [14]. The following augmentations were used:

- Gamma intensity transformation.
- Rotation - Maximum angle: 10 degrees.
- Gaussian shadows - Dark shadows applied to the image at random locations and with random sizes.
- Depth - Cuts the image bottom at random depths.
- JPEG compression - Compresses the image with a random quality setting.
- Elastic image deformation.

D. Real-time application

A real-time application was created using FAST¹ [17], [18], a framework for GPU-based high-performance image processing and visualization, and the Clarius Cast research toolkit² which can be used to stream ultrasound images from

¹<https://fast.eriksmistad.no>

²<https://github.com/clariusdev/cast/>

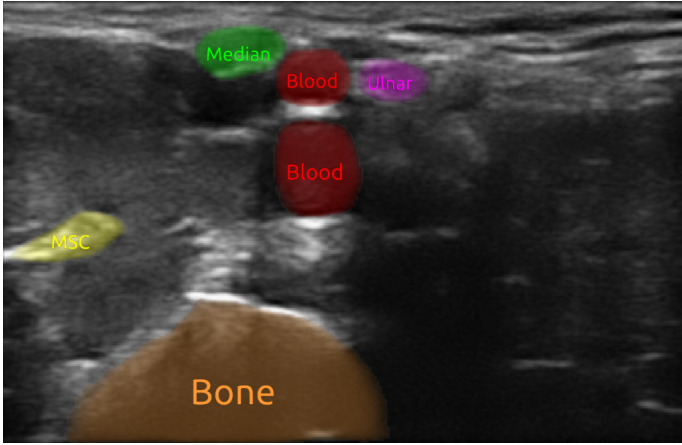


Fig. 3. Example of an ultrasound axillary image segmented and visualized in real-time with FAST.



Fig. 5. Real-time prototype consisting of a FAST application, a Surface Book laptop and a Clarius L15 HD scanner.

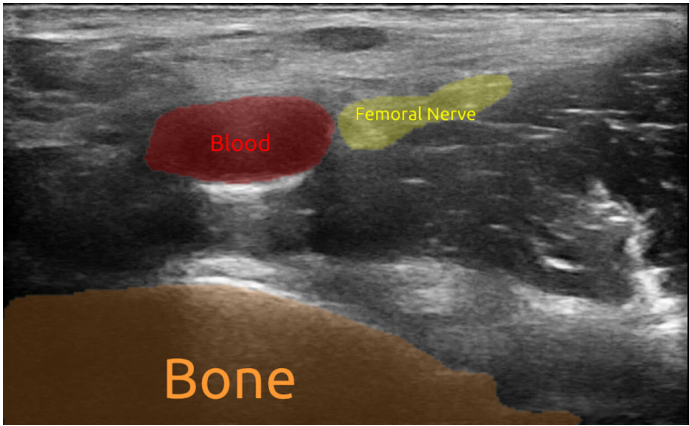


Fig. 4. Example of an ultrasound femoral image segmented and visualized in real-time with FAST.

Clarius ultrasound scanners while scanning. The prototype consists of a Surface Book laptop and a Clarius L15 HD scanner as shown in Fig. 5. Ultrasound images are streamed over a WiFi hotspot created by the scanner. The segmentation results were visualized with FAST using transparent colors and text labels on top of the ultrasound images as shown in figures 3-5.

E. Evaluation

Since precise detection is more important in this application than exact delineation of the structures, precision, recall and F1 scores were calculated for every structure. A segmentation region was counted as a true positive if there was more than 25% overlap with the true segmentation, the same as used in [14]. Segmentation regions smaller than a circle of 7 pixels radius were ignored. The Dice similarity metric was also calculated for all structures. 10-fold cross validation was used to calculate the performance on the entire dataset.

III. RESULTS

The F1 detection scores of the musculocutaneous (MSC), median and ulnar nerves as well as blood vessels and bone

for the axillary nerve block were 0.72, 0.84, 0.54, 0.85, 0.91 respectively. For the femoral nerve block, the accuracy for the femoral nerve, blood vessels and bone were 0.79, 0.90, 0.78. The Dice scores were 0.56, 0.57, 0.51, 0.72, 0.74 and 0.46, 0.85, 0.27 for the axillary and femoral nerve blocks respectively. Figures 1 and 2 shows bar plots of the F1 score, recall, precision and dice for each structure of the axillary and femoral nerve blocks respectively. Figures 3 and 4 shows a segmentation example of an axillary and femoral ultrasound image visualized with FAST. The real-time application developed (Fig. 5) was able to stream, process and visualize the results in real-time using about 31 ms per frame on a laptop with a GTX 1060 GPU.

IV. DISCUSSION

The results show a large variation in detection accuracy for different nerves. For instance, the median nerve is detected with an F1 score of 0.84, while the ulnar nerve is detected with an F1 score of 0.54. This illustrates the challenge of segmenting nerves; their appearance and visibility varies a lot depending on the surrounding tissue which interferes with the ultrasound waves. Due to these variations, transfer learning for segmenting nerves from different areas of the body may not improve results, and comparing segmentation accuracy of different nerves may not be reasonable because some nerves are easier to get a good ultrasound image of than others. The detection performance for blood vessels and bone is quite high, although detection of these structures can also be challenging in patients with more body fat as this reduces ultrasound image quality and increases the distance between the ultrasound probe and the structures to be imaged.

Based on our experience, the MSC nerve is usually surrounded by muscle tissue in the image and therefore often appear as a clear hyperechoic structure surrounded by hypoechoic muscle tissue. Still, there are other structures which

appear similar and thus may contribute to the slightly lower F1 score of 0.72 compared to the median and femoral nerve. The median nerve does not always appear hyperechoic, but is often located near the axillary artery which is easily detected. This may have contributed to the high median accuracy. The ulnar nerve is less distinct and clear, and often surrounded by veins and thus the most difficult nerve to find among the nerves targeted in this work.

The femoral nerve is a large nerve often located close to the large femoral artery resulting in high F1 scores. Although the F1 score of the femoral nerve was high (0.79), the Dice score was low (0.46), this may be the result of this nerve being larger than the other nerves. One can also observe a much larger standard deviation on the femoral nerve block in Fig. 2 compared to the axillary nerve block in Fig. 1. This is most likely because only data from 20 subjects were used for training the femoral nerve block models, while data from over 100 subjects were used for the axillary models. Transfer learning from the axillary model was tested, but did not give any significant performance improvement.

The neural networks used in this work only segment one frame at a time, thus the networks have no temporal memory. Humans, on the other hand, look at an ultrasound sequence when interpreting these images. Studying the dynamics and speckle patterns of the ultrasound image sequence aids considerably in interpretation of the ultrasound images. Thus, future work should include looking into temporal neural networks for ultrasound segmentation as recently explored by several groups [19], [20].

V. CONCLUSION

Deep neural networks were trained to segment nerves, blood vessels and bone in ultrasound images from the armpit and groin. The results showed a large variation in detection performance for different nerves, illustrating the fact that some nerves are better visualized with ultrasound imaging than others. The networks were used to develop a prototype which was able to stream, segment and visualize ultrasound images while highlighting and labeling the nerves, blood vessels and bone in real-time using a laptop and a Clarius L15 ultrasound scanner.

REFERENCES

- [1] B. S. Worm, M. Krag, and K. Jensen, “Ultrasound-Guided Nerve Blocks - Is Documentation and Education Feasible Using Only Text and Pictures?” *PLoS ONE*, vol. 9, no. 2, pp. 1–7, 2014.
- [2] J. T. Wegener, C. T. Van Doorn, J. H. Eshuis, M. W. Hollmann, B. Preckel, and M. F. Stevens, “Value of an electronic tutorial for image interpretation in ultrasound-guided regional anaesthesia,” *Regional Anesthesia and Pain Medicine*, vol. 38, no. 1, pp. 44–49, 2013.
- [3] O. Hadjerci, A. Hafiane, P. Makris, D. Conte, P. Vieyres, and A. Delbos, “Nerve Detection in Ultrasound Images Using Median Gabor Binary Pattern,” in *11th International Conference, ICIAR 2014*, 2014, pp. 132 – 140.
- [4] ———, “Nerve Localization by Machine Learning Framework with New Feature Selection Algorithm,” in *Lecture Notes in Computer Science (including subseries Lecture Notes in Artificial Intelligence and Lecture Notes in Bioinformatics)*, 2015, vol. 9279, no. July, pp. 246–256.
- [5] O. Hadjerci, A. Hafiane, D. Conte, P. Makris, P. Vieyres, and A. Delbos, “Computer-aided detection system for nerve identification using ultrasound images: A comparative study,” *Informatics in Medicine Unlocked*, vol. 3, no. June, pp. 29–43, 2016.
- [6] A. Hafiane, P. Vieyres, and A. Delbos, “Phase-based probabilistic active contour for nerve detection in ultrasound images for regional anesthesia,” *Computers in Biology and Medicine*, vol. 52, pp. 88–95, 2014.
- [7] E. Smistad, D. H. Iversen, L. Leidig, J. B. Lervik Bakeng, K. F. Johansen, and F. Lindseth, “Automatic Segmentation and Probe Guidance for Real-Time Assistance of Ultrasound-Guided Femoral Nerve Blocks,” *Ultrasound in Medicine and Biology*, vol. 43, no. 1, pp. 218–226, 2017.
- [8] P. Abolmaesumi, M. Sirospour, and S. Salcudean, “Real-time extraction of carotid artery contours from ultrasound images,” in *Proceedings 13th IEEE Symposium on Computer-Based Medical Systems. CBMS 2000*. IEEE Comput. Soc., 2000, pp. 181–186.
- [9] J. Guerrero, S. E. Salcudean, J. A. McEwen, B. A. Masri, and S. Nicolaou, “Real-time vessel segmentation and tracking for ultrasound imaging applications,” *IEEE Transactions on Medical Imaging*, vol. 26, no. 8, pp. 1079–1090, 2007.
- [10] E. Smistad and F. Lindseth, “Real-Time Automatic Artery Segmentation, Reconstruction and Registration for Ultrasound-Guided Regional Anaesthesia of the Femoral Nerve,” *IEEE Transactions on Medical Imaging*, vol. 35, no. 3, pp. 752–761, 3 2016.
- [11] H. Zhao and N. Sun, “Improved U-Net Model for Nerve Segmentation,” in *ICIG 2017*, ser. Lecture Notes in Computer Science, Y. Zhao, X. Kong, and D. Taubman, Eds. Cham: Springer International Publishing, 2017, vol. 10666, pp. 496–504.
- [12] M. Baby and A. S. Jereesh, “Automatic nerve segmentation of ultrasound images,” in *Proceedings of the International Conference on Electronics, Communication and Aerospace Technology, ICECA 2017*, 2017, pp. 107–112.
- [13] E. Smistad and L. Lovstakken, “Vessel Detection in Ultrasound Images Using Deep Convolutional Neural Networks,” in *DLMIA*, ser. Lecture Notes in Computer Science, G. Carneiro, D. Mateus, L. Peter, A. Bradley, J. M. R. S. Tavares, V. Belagiannis, J. P. Papa, J. C. Nascimento, M. Loog, Z. Lu, J. S. Cardoso, and J. Cornebise, Eds., vol. 10008. Cham: Springer International Publishing, 2016, pp. 30–38.
- [14] E. Smistad, K. F. Johansen, D. H. Iversen, and I. Reinertsen, “Highlighting nerves and blood vessels for ultrasound-guided axillary nerve block procedures using neural networks,” *Journal of Medical Imaging*, vol. 5, no. 04, p. 1, 11 2018.
- [15] E. Smistad, A. Østvik, and L. Lovstakken, “Annotation Web - An open-source web-based annotation tool for ultrasound images,” in *IEEE International Ultrasonics Symposium, IUS*, 2021.
- [16] O. Ronneberger, P. Fischer, and T. Brox, “U-Net: Convolutional Networks for Biomedical Image Segmentation,” *MICCAI*, pp. 234–241, 2015.
- [17] E. Smistad, M. Bozorgi, and F. Lindseth, “FAST: framework for heterogeneous medical image computing and visualization,” *International Journal of Computer Assisted Radiology and Surgery*, vol. 10, no. 11, pp. 1811–1822, 2015.
- [18] E. Smistad, A. Østvik, and A. Pedersen, “High Performance Neural Network Inference, Streaming and Visualization of Medical Images using FAST,” *IEEE Access*, vol. 7, pp. 1–1, 2019.
- [19] M.-H. Horng, C.-W. Yang, Y.-N. Sun, and T.-H. Yang, “DeepNerve: A New Convolutional Neural Network for the Localization and Segmentation of the Median Nerve in Ultrasound Image Sequences,” *Ultrasound in Medicine & Biology*, vol. 00, no. 00, pp. 1–14, 6 2020.
- [20] E. Smistad, I. M. Salte, H. Dalen, and L. Lovstakken, “Real-time temporal coherent left ventricle segmentation using convolutional LSTMs,” in *IEEE International Ultrasonics Symposium, IUS*, 2021.